

CIRCUMSTELLAR GAS AROUND 51 OPHIUCHI

A. Johnson

University of California, Santa Cruz, CA, 95064

Abstract. Presented is the examination of HST STIS data collected for the Be star 51 Ophiuchi. This system is thought to be similar to that of the well-studied β Pictoris, containing a disk of gas and dust orbiting a parent star. Such debris disks are thought to be young planetary systems; additional information about the gas abundances of such disks may lead to a better understanding of how planets form around stars. Lower limits to the column densities for Fe II, Ni II, Cr II, and N I were calculated from the circumstellar absorption lines' measured equivalent widths, assuming the lines were not optically thick. The CS gas was found to have a mean velocity of $-16.9 \pm 0.8 \text{ km s}^{-1}$; velocities for individual transitions toward the star are also presented.

1. Introduction

51 Ophiuchi (HD158643) is a young Be star with an age of about 0.3 My (van den Ancker, de Winter, & Tjin A Djie 1998). Coté and Waters (1987) were the first to detect an infrared excess around this star, from which the existence of a circumstellar disk was inferred. The first evidence for accreting gas around a star other than β Pic was subsequently presented for 51 Ophiuchi by Grady and Silvis (1993). Roberge et al (2008) also found in the star's UV spectrum redshifted and variable absorption lines thought to indicate infalling circumstellar material. Such findings have led to the likening of the 51 Oph disk to that of β Pictoris, a system thought to be in the later stages of planet formation (Lecavelier et al., 2001). Studying β Pic-like stars such as 51 Oph may lead to a clearer scientific picture of the planet formation process.

An important mystery yet to be solved is the composition of the gas component of the 51 Oph disk. Roberge (2008) measured the variable component of the gas; this included detections of N I, N II, and Fe III. Le Cavalier de Etangs et al (1997) found C I absorption in the UV spectrum, and others (van den Ancker 2001; W.-F. Thi 2005) have even found indications of large amounts of molecular gas in the IR. An examination of the bulk, line-of-sight abundances has not yet been conducted, and will help to accurately determine the composition of the circumstellar gas. The STIS UV spectrum of 51 Ophiuchi gathered by Alain le Cavalier de Etangs et al exhibits myriad narrow circumstellar absorption lines. This absorption-rich spectrum is an

opportune place to extract such information about the star's gaseous circumstellar environment.

A task under the data analysis software IRAF called 'splot' was used to fit profiles to the CS absorption lines and return values for equivalent width, line center, FWHM for the fitted profile, and corresponding errors. Several atomic line databases were queried to identify the lines, including NIST, Kurucz, and the Atomic Line List. Column densities for the species were calculated from the measured equivalent widths, assuming an optical depth $\tau \ll 1$. Since this assumption is probably not entirely correct, the calculated column densities are likely lower limits to the actual values.

2. Data

A data request form was submitted to the Space Telescope Data Archive (STDADS) through MAST to retrieve the UV spectrum of 51 Ophiuchi. These HST observations were conducted on 26 May 2003 using echelle gratings E140H and E230H on the STIS instrument. The full UV spectrum of 51 Oph is split into six data sets, or observations, executed at different times and wavelengths. Each set itself contains anywhere from 30 to 70 partially overlapping echelle orders of about 10 angstroms in length. Figure 2 displays a low-resolution preview of the co-added first five data sets for the star (the sixth set covers an island of wavelengths $\sim \lambda\lambda 2576.6$ - 2845.8 and has not yet been measured). The aperture configurations used were 0.2×0.2 and 0.1×0.3 pixels yielding a spectral resolution of ~ 1 pixel FWHM at these UV wavelengths. This was sufficient to resolve the CS absorption lines in the spectrum.

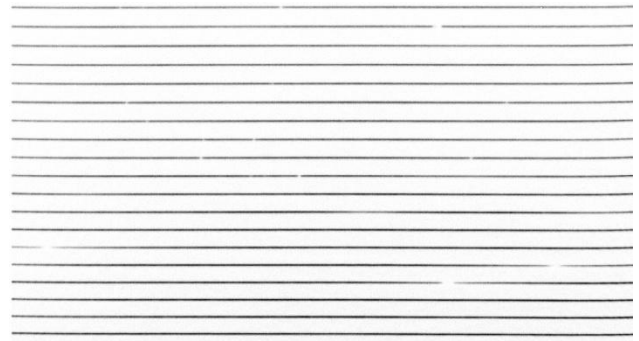


Figure 1: Segment of Raw STIS Echelle Data for 51 Ophiuchi

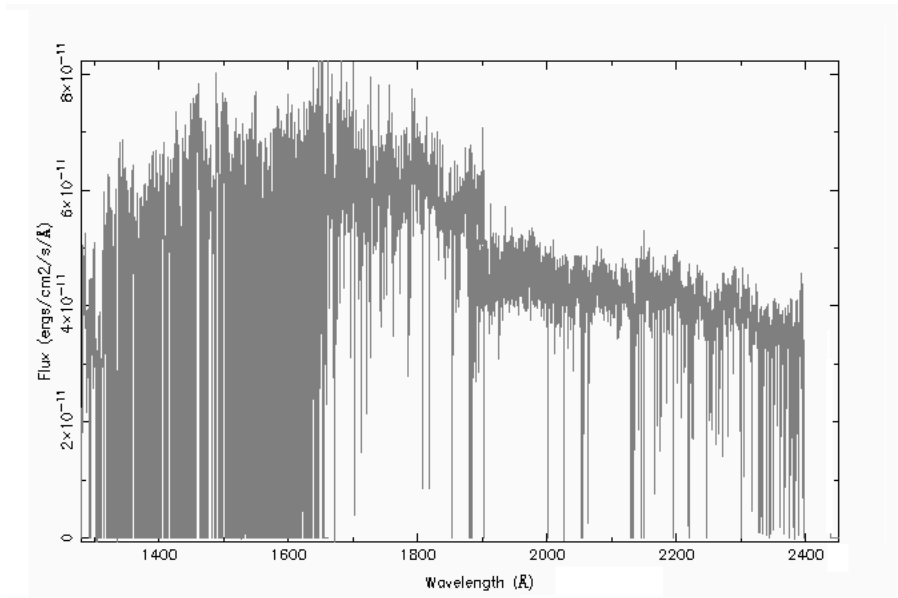


Figure 2: Low-resolution Coadd Plot of Reduced 51 Ophiuchi Spectrum

3. Methods

3.1 Measurements

The Image Reduction and Analysis Facility (IRAF) is software for the reduction and analysis of astronomical data. The IRAF command ‘tomultispec’ was used to convert the retrieved x1d.fits files (the fits files containing the reduced spectrum) into the old .imh and .pix format. This was then written into the modern .fits format using the command ‘wfits’ (write fits).

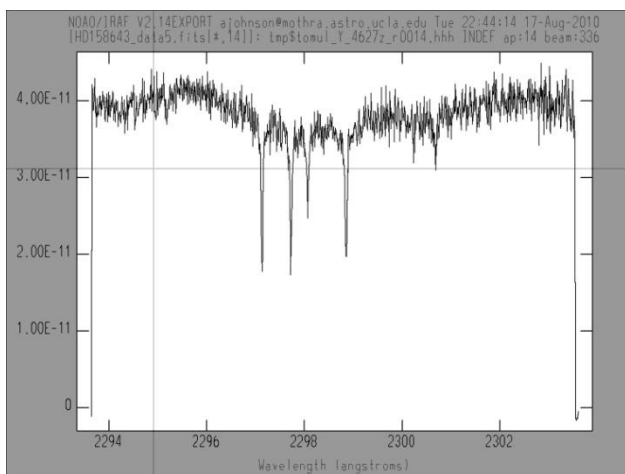


Figure 3: IRAF Snapshot of CS Ni II Absorption Lines

The IRAF task ‘splot’ supports deblending, the fitting of Gaussian, Lorentzian, or Voigt profiles to absorption lines. Once a profile is fit to a line, values for equivalent width and center wavelength of the line, the FWHM of the profile, and the continuum intensity at line center can be returned upon request. Each line was measured several times to get the best possible value for equivalent width. A total of 182 lines were measured, excluding duplicates and small lines (equivalent width less than 10mÅ).

3.2 Line Identification

Transitions were identified using multiple atomic line databases. These included a table created to identify lines in the UV spectrum of η Carinae (Nielsen et al 2003), the NIST atomic spectra database, the Atomic Line List hosted by U of Kentucky, the R. L. Kurucz database, and a list assembled by D. Koester with data mainly from the Vienna Atomic Line Database. Several transition lines were assigned identifications that could not be easily ascertained. For instance, a line at λ1414.324 had no other reasonable identification than a ground-state Ga II transition. This wavelength corresponds to the strongest such Ga II transition. Since this line is already small (~10mÅ), no other Ga II lines are expected to appear in the spectrum; this makes the identification difficult to confirm. Similar situations arose for Cl I, Si II, and Zn II transitions.

3.3 Velocity and Column Density Calculations

The velocity at which a particular ion moves as it emits a photon can be measured by applying the Doppler effect formula for light.

$$\frac{\Delta\lambda}{\lambda} = \frac{v}{c}$$

Where $\Delta\lambda$ is the difference between the observed wavelength and expected laboratory wavelength and λ is the lab wavelength.

Column density is a measure of the abundance of a species toward an astronomical object given by the integral of its density along the line of sight. It can also be calculated by measuring the equivalent widths of absorption lines in the star's spectrum.

$$N_L = \frac{m_e c^2}{\pi e^2 \lambda^2 f} W_\lambda$$

The column density N_L corresponding to a particular absorption line is given by this relation, which depends on the equivalent width of the line W_λ (a measure of the area of the absorption line), its center wavelength λ , and the oscillator strength of that transition f . Transition strengths were retrieved from mentioned atomic line databases.

3.4 Error Calculations

Given a measure of a spectrum's noisiness, 'splot' can assess the inherent measurement error for each equivalent width value it returns. An equally noteworthy error is that arising from the user's input. To fit a profile, the user must mark two positions along the continuum of the spectrum, one on either side of an absorption line. Often a circumstellar line is superimposed on some other absorption feature, however, and identifying the continuum becomes non-trivial. In order to account for the uncertainty of this process, several measurements were made for each individual line. For the first, a Lorentzian was fit, and the continuum interval was selected ~0.5-1.0 angstrom on either side of the center of the absorption line. A Voigt profile was fit next, this time fitting any broad, superimposed stellar features with the narrow CS line. Finally, several direct sums over the flux across the absorption line were averaged to check the profile measurements. Standard deviations of the three measurements (Lorentz, Voigt, direct sum) were calculated to evaluate the errors involved in choosing specific profiles and continuums. The two sources of equivalent width error were then combined (added in quadrature) and propagated to get the column density error. Since often column densities for multiple lines in a given energy level were measured—and are expected to

be the same—the standard deviation of these measurements was incorporated into the total error for column density (the magnitude of this error was usually close to the measurement error).

4. Results

4.1 Velocities

The histogram shown in Figure 4 describes the distribution of transition velocities in the 51 Oph spectrum. This distribution reveals a prominent velocity structure centered between -17 km s^{-1} and -16.5 km s^{-1} and possibly a smaller one centered at about -20 km s^{-1} . The mean velocity is -16.9 km s^{-1} with a mean deviation of $\sim 0.8 \text{ km s}^{-1}$.

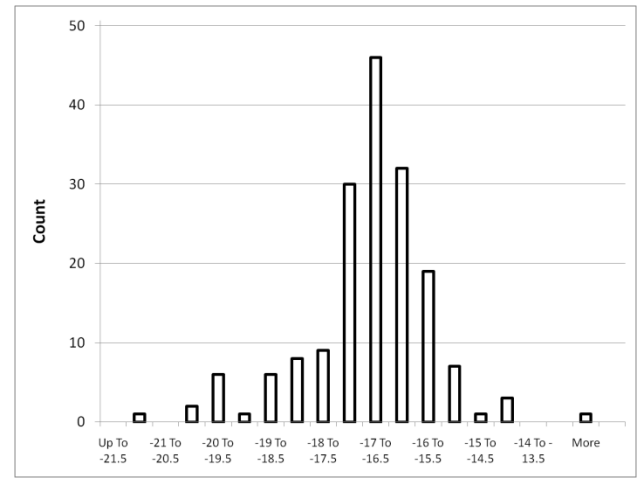


Figure 4: Histogram of Transition Velocities in km s^{-1}

4.2 Column Densities

Table 1 shows lower limits to the total column densities for the different species found in the STIS spectrum of 51 Ophiuchi. Table 2 shows the populations of the various energy levels for each species.

Species	N_L ($\times 10^{13} \text{ cm}^{-2}$)
Cl I*	3.3 ± 0.3
Cr II	0.6 ± 0.1
Fe II	143.6 ± 11.1
Ga II*	0.03 ± 0.01
N I	10.3 ± 1.3
Ni II	5.5 ± 0.8
Si II*	154.7 ± 21.8
Zn II*	0.8 ± 0.1

Table 1: CS Species in the STIS Spectrum of 51 Oph

*Questionable identification—not enough lines to be sure.

5. Concluding Remarks

The STIS UV spectrum of 51 Ophiuchi was found to contain unexpected ions as well as unusually high Fe II excitation levels. The observed Cl I and Ga II are interesting and curious species to find in the star's circumstellar disk. If their identifications hold it will be interesting to ask where they come from. The measured total column density for N I was $10.3 \pm 1.3 \times 10^{13} \text{ cm}^{-2}$. Roberge et al (2008) found it to be $5.84 \pm 1.1 \times 10^{13} \text{ cm}^{-2}$ (measuring FUSE data 3 years older than that from STIS). No N II, O I, or Fe III was observed in the STIS spectrum.

LeCavalier et al (1996) found for 51 Oph's radial velocity a value of $-17 \pm 3 \text{ km/s}$. More recently, Roberge lists the star's heliocentric velocity to be $-21 \text{ km s}^{-1} \pm 14 \text{ km s}^{-1}$. Given these values no velocity relative to the star can be deduced for the CS gas ($v = -16.9 \pm 0.8 \text{ km s}^{-1}$).

It might also be worthwhile to note what appears to be an additional velocity structure centered at $\sim -20 \text{ km s}^{-1}$. The calculated column density for ground state Fe II comes with an abnormally large error arising from a large dispersion of values given by different absorption lines. Half the ground state Fe II lines appear to center around -20.3 km s^{-1} and the other half at -17.9 km s^{-1} ; the error is greatly reduced if the Fe II is resolved into these two structures. The corresponding column densities for these structures are $7.5 \pm 3.9 \times 10^{13} \text{ cm}^{-2}$ and $39.2 \pm 6.0 \times 10^{13} \text{ cm}^{-2}$, respectively. Whether additional ions contribute to this feature or it appears by chance is unclear and left for further work.

This examination should bring new pieces to the 51 Ophiuchi puzzle, but there is plenty more to learn about this potentially planet forming system. More work is to be done with the STIS UV spectrum, including measurement of a rich sixth data set and a more detailed analysis of the CS absorption lines.

References

- van den Ancker M.E., de Winter D., Tjin A Djie H.R.E., 1998, A&A 330, 145
Coté J., Waters L.B.F.M., 1987, A&A 176
Grady, C. A. & Silvis, J. M. S. 1993, A&A, 420, L61
Roberge, A., Feldman, P. D., Lecavelier des Etangs, A., Vidal-Madjar, A., Deleuil, M., Bouret, J.-C., Ferlet, R., & Moos, H. W. 2002, ApJ, 568, 343
Lecavelier des Etangs A., Vidal-Madjar A., Backman D.E., et al., 1997, A&A 321, L39
Lecavelier et al., 2001, Nature 412, 706
van den Ancker, M. E., Meeus, G., Cami, J., Waters, L. B. F. M., & Waelkens, C. 2001, A&A, 369, L17
W.-F. Thi, B. van Dalen, A. Bik, and L. B. F. M. Waters. 2008, A&A.

TABLE 2
ENERGY LEVEL POPULATIONS IN THE CS GAS AROUND 51 OPHIUCHI

Species	Lower Energy Level (cm ⁻¹)	N _L (×10 ¹³ cm ⁻²)	Velocity [†] (km s ⁻¹)
Cl I*	0	2.3 ± 0.3	-15.9
Cl I	879	0.95 ± 0.1	-16.4
Cr II	0	0.6 ± 0.1	-16.6
Fe II	0	23.38 ± 17.9**	-19.1
Fe II	385	8.6 ± 5.5	-16.9
Fe II	668	29.1 ± 3.8	-17.1
Fe II	863	5.0 ± 2.0	-18.1
Fe II	977	2.7 ± 0.2	-18.8
Fe II	1036	0.8 ± 0.1	-17.5
Fe II	1873	8.9 ± 3.1	-17.3
Fe II	2430	6.2 ± 1.9	-16.8
Fe II	2838	5.2 ± 1.5	-17.3
Fe II	3117	3.4 ± 1.0	-17.2
Fe II	7955	6.1 ± 0.7	-17.0
Fe II	8392	3.8 ± 1.2	-18.1
Fe II	8680	2.7 ± 0.5	-18.9
Fe II	8847	1.0 ± 0.3	-17.8
Fe II	13474	1.1 ± 0.2	-16.6
Fe II	15845	1.3 ± 0.7	-16.6
Fe II	15847	0.2 ± 0.02	-17.2
Fe II	16369	1.4 ± 0.3	-16.3
Fe II	18361	0.7 ± 0.2	-16.0
Fe II	20340	1.5 ± 0.4	-16.4
Fe II	20806	0.9 ± 0.4	-16.2
Fe II	21252	1.4 ± 0.3	-15.4
Fe II	21430	1.4 ± 0.3	-17.3
Fe II	21582	1.3 ± 0.3	-17.4
Fe II	21712	1.2 ± 0.3	-16.7
Fe II	23318	0.2 ± 0.03	-15.0
Fe II	26170	0.9 ± 0.2	-17.8
Ga II*	0	0.03 ± 0.01	-16.5
N I	19224	4.4 ± 1.0	-16.3
N I	19233	3.8 ± 0.7	-15.8
N I	28839	2.1 ± 0.5	-16.3
Ni II	0	1.5 ± 0.6	-16.9
Ni II	1507	0.3 ± 0.1	-14.2
Ni II	8394	0.9 ± 0.2	-16.5
Ni II	9330	0.8 ± 0.2	-16.3
Ni II	10116	0.5 ± 0.2	-16.0
Ni II	10664	0.4 ± 0.1	-16.0
Ni II	13550	0.4 ± 0.1	-15.2
Ni II	14996	0.6 ± 0.3	-16.0
Si II*	0	64.5 ± 6.9	-18.2
Si II*	287	90.2 ± 20.6	-17.5
Zn II*	0	0.8 ± 0.1	-18.1

[†] Average velocity of species in this energy level.

*Questionable identification—not enough lines to be sure.

**Abnormally large error may be due to additional Fe II structure in gas (see discussion on velocity structure at -20 km s⁻¹).

